Inorganic Chemistry

pubs.acs.org/IC Article

Ferrocene-Functionalized Crystalline Biomimetic Catalysts for Efficient CO_2 Photoreduction

Su-Juan Yao,[⊥] Ning Li,[⊥] Jiang Liu,* Long-Zhang Dong, Jing-Jing Liu, Zhi-Feng Xin, Dong-Sheng Li, Shun-Li Li, and Ya-Qian Lan*

Cite This: *Inorg. Chem.* 2022, 61, 2167−2173 Read Online

ACCESS | Metrics & More | Article Recommendations | Supporting Information

Downloaded via NANJING NORMAL UNIV on March 10, 2022 at 01:51:29 (UTC).
See https://pubs.acs.org/sharingguidelines for options on how to legitimately share published articles.

ABSTRACT: Photoreducing carbon dioxide (CO_2) into highly valued chemicals or energy products has been recognized as one of the most promising proposals to degrade atmospheric CO_2 concentration and achieve carbon neutrality. Adenine with a photosensitive amino group and aromatic nitrogen atom can strongly interact with CO_2 and has been authenticated for its catalytic activity for the CO_2 photoreduction reaction (CO_2RR). Herein, two adenine-constructed crystalline biomimetic photocatalysts (Co_2-AW and Co_2-AF) were designed and synthesized to achieve CO_2RR. Between them, Co_2-AF displayed higher photocatalytic activity (225.8 μmol g^{-1} h^{-1}) for CO_2-to-HCOOH conversion than that of Co_2-AW. It was found that the superior charge transfer capacity of the functional ferrocene group in Co_2-AF is the primary reason to facilitate the photocatalytic performance efficiently. Additionally, this work also demonstrated the great potential of the ferrocene group as an electron donor and mediator in improving the photocatalytic activity of crystalline coordination catalysts.

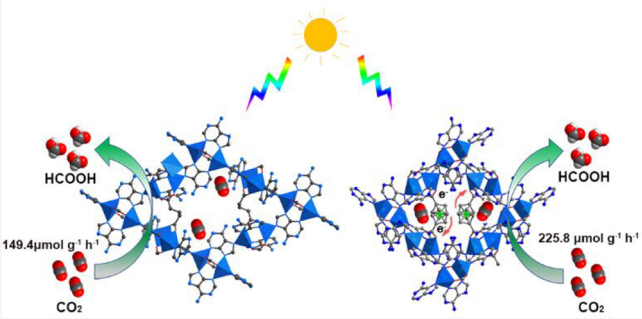

■ INTRODUCTION

Biomolecules are the building blocks of life. Biologically and environmentally compatible organic molecules as ligands to construct biomimetic metal−organic frameworks (BMOFs) have been widely used in the fields of biological applications,[1−5] catalysis,[6−13] CO_2 capture,[14,15] separation,[16−18] sensing,[19] etc. BMOFs have been promising materials for their accessibility (low toxicity) and bonding ability.[20,21] For example, nucleobases considered as attractive sorts of bio-organic ligands have led to the formation of biomimetic porous materials for their rich coordination nitrogen donor sites of different basicities,[22,23] which provide a multidentate coordination environment and a variety of structures; and beyond that, nucleobases chelated in the building units have multiple coordination positions,[24,25] including an N atom from purine, pyrimidine, or the substituted amino group. The multiple coordination sites and binding modes can interact with metals to generate biomimetic metal−organic clusters/chains/sheets/frameworks, along with abundant hydrogen bonds and $\pi-\pi$ stacking interactions.[26,27] Consequently, making them ideal biomimetic organic ligands to construct multiple structural BMOFs is attributed to their rigid entity, abundant coordination sites, numerous hydrogens, and $\pi-\pi$ stacking interactions.

Under this circumstance, adenine is selected as the suitable linker to assemble BMOFs. Adenine contains five nitrogen donor sites of different basicities that make them attractive ligands for metal coordination in mono-, bi-, tri-, or tetradentate coordination patterns for the composition of BMOFs.[28,29] Moreover, its rigid molecular structure and versatile metal coordination modes make it possible as an organic linker for porous BMOFs.[30] In addition to the possible role that adenine plays in the conformational and functional properties of BMOFs, it is also beneficial for CO_2 capture and activation.[31−33] In particular, the uncoordinated nitrogen donor sites (N) and amino group N constitute Watson−Crick active sites, which are regarded as Lewis base sites, and can interact with CO_2.[34]

Visible-light driven CO_2 conversion had been an effective approach to achieve a green, circular, and sustainable ecological environment.[35−43] The biomimetic molecules, due to their biological and environmental compatibility, have been used for CO_2 reduction.[44−49] Taking advantage of these features, two low-toxicity BMOFs, $[Co_2(HAD)_2(AD)_2(GA)]$ (Co_2-AW, GA = glutaric acid) and $[Co_2(HAD)_2(AD)_2(FA)]$ (Co_2-AF, FA = 1,1′-ferrocenedicarboxylic acid), were constructed by selecting HAD, GA, and FA as organic linkers. Co_2-

Received: October 28, 2021
Published: January 13, 2022

© 2022 American Chemical Society

https://doi.org/10.1021/acs.inorgchem.1c03368
Inorg. Chem. 2022, 61, 2167−2173

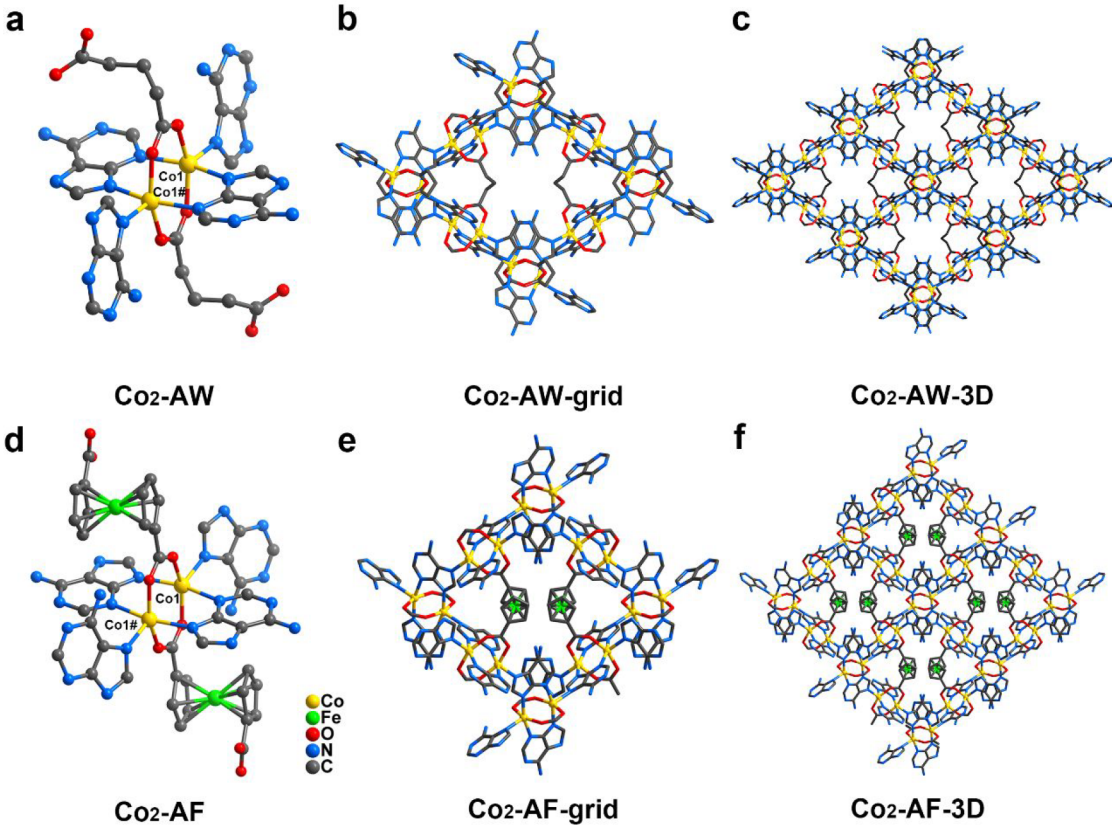

Figure 1. (a, d) The PWU of **Co_2-AW** and **Co_2-AF**. (b, e) The crystal structures of **Co_2-AW** and **Co_2-AF**. (c, f) Three-dimensional microporous networks of **Co_2-AW** and **Co_2-AF**.

AW and Co_2-AF are similar metal−organic frameworks constructed by GA and FA, respectively. These two BMOFs were used as catalysts for photocatalytic CO_2RR based on the photosensitive amino group and Lewis base sites on the HAD molecule, which is beneficial for the capture and activation of CO_2. The photocatalytic results reveal that these two BMOFs exhibit highly photocatalytic selectivity for CO_2-to-HCOOH conversion. Between them, Co_2-AF displayed higher photocatalytic activity (225.8 μmol g^{-1} h^{-1}), which was higher than that of Co_2-AW (149.4 μmol g^{-1} h^{-1}). The high photocatalytic property is mainly ascribed to the HAD ligands in BMOFs structures, which act as light absorbing units with CO_2 adsorption and catalytic activation sites. Moreover, Co_2-AF showed higher photocatalytic activity than that of homomorphous Co_2-AW, probably due to the strong charge transfer capacity of the functional ferrocene group.[50−52] Significantly, this work affords an enlightenment to design and develop high-performance biomimetic photocatalysts for CO_2RR.

■ EXPERIMENTAL SECTION

Synthesis of Co_2-AW. **Co_2-AW** was synthesized among 0.1 mmol of $Co(ClO_4)_2$, 0.3 mmol of adenine, and 0.3 mmol of glutaric acid in the presence of 6 mL of DMF by a solvothermal reaction. The solution was stirred for 30 min to dissolve and heated in a 150 °C oven for 3 d. After cooling down naturally, dark octahedron crystals were obtained.

Synthesis of Co_2-AF. **Co_2-AF** was synthesized among 0.1 mmol of $Co(ClO_4)_2$, 0.3 mmol of adenine, and 0.2 mmol of 1,1′-ferrocenedicarboxylic acid in the presence of 4 mL of DMF and 2 mL of isopropyl alcohol by a solvothermal reaction. The solution was stirred for 30 min to dissolve and heated in a 120 °C oven for 6 d. After cooling down naturally, orange octahedron crystals were obtained.

■ RESULTS AND DISCUSSION

Single-crystal X-ray diffraction analysis reveals that Co_2-AW and Co_2-AF crystallize in the tetragonal space group $I4_1/a$ (Tables S1−S3) with an asymmetric unit consisting of one Co ion, one AD^- ligand, and one-half of a GA molecule for Co_2-AW or an FA molecule for Co_2-AF. The crystallographically independent Co1 ion of Co_2-AW is five-coordinated, which links two carboxyl oxygen atoms (O1 and O2) of two distinct GA ligands and two adenine imidazole N atoms (N1 and N2) and one adenine aromatic group N atom (N3) (Figure S2), exhibiting a distorted tetrahedral pyramid coordination geometry. Each HAD ligand connects three Co1 atoms using three N atoms (N1, N2, and N3) (Figure S1); the naked N4 and N5 atoms of adenine are pointing toward the inner portion of the channels and act as Watson−Crick active sites that can adsorb CO_2 molecules. Two nearby Co1 atoms, linked with two GA and two HAD ligands, form a paddle wheel unit (PWU) (Figures 1a and S3) and per PWU connect six adjacent PWUs to generate a three-dimensional (3D) framework through the N atoms on HAD ligands and a carboxyl oxygen of GA (Figure 1b,c). Replacement of GA in Co_2-AW by FA (with strong charge transfer ability) can generate a nearly isostructural 3D entity, Co_2-AF (Figures 1d−f and S4−S6). The coordination environment of these two BMOFs is the same. The coordinated FA ligand as a strong electron transporter in Co_2-AF can promote efficient charge transfer.

https://doi.org/10.1021/acs.inorgchem.1c03368
Inorg. Chem. 2022, 61, 2167−2173

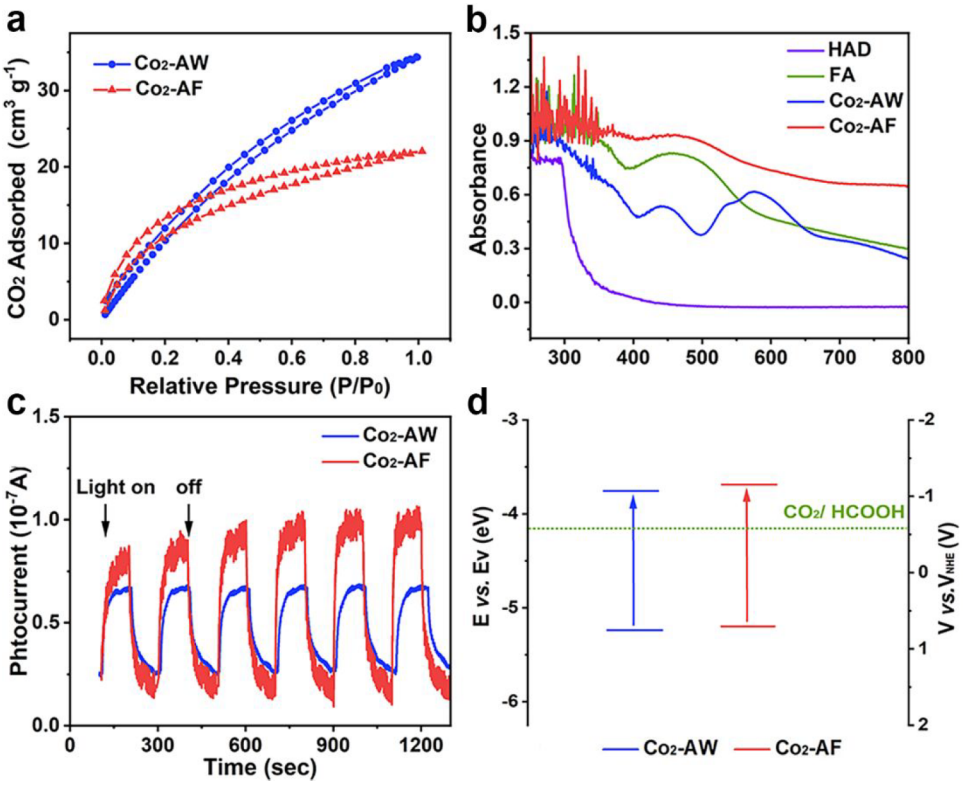

Figure 2. (a) CO_2 adsorption isotherms of **Co_2-AW** and **Co_2-AF** at 298 K. (b) UV−vis absorption spectra of **HAD**, **FA**, **Co_2-AW**, and **Co_2-AF**. (c) Transient photocurrent responses of **Co_2-AW** and **Co_2-AF**. (d) The energy band structure diagram for **Co_2-AW** and **Co_2-AF**.

Powder X-ray diffraction (PXRD) patterns for Co_2-AW and Co_2-AF were in accordance with their simulated patterns (Figures S7 and S8), revealing that all the complexes have good crystallinity and phase purity. Chemical stability of Co_2-AW and Co_2-AF was checked under diverse conditions. As shown in Figure S9, the Co_2-AW structure was maintained very well under all the tested solvent systems and the crystalline structure of Co_2-AF did not show remarkable regression after long-term immersion with reaction solvents (Figure S10). Thermogravimetric analysis (TGA) of Co_2-AW and Co_2-AF was implemented under an N_2 atmosphere to investigate their thermal stability (Figure S11). The CO_2 adsorption isotherms of activated Co_2-AW and Co_2-AF were measured and determined to be 34 and 22 cm^3 g^{-1} (Figure 2a), and N_2 adsorption isotherms and pore-size distribution were shown in Figure S12. Since effective absorption of sunlight is the primary condition for photocatalysis, ultraviolet visible (UV−vis) absorption spectra of these two BMOFs were performed. UV−vis absorption spectrum of Co_2-AW and Co_2-AF demonstrated that all the BMOFs exhibited broad and obvious visible light absorption compared with the HAD molecule (Figure 2b). The strong UV−vis absorption range of these BMOFs was mainly attributed to the incorporation of auxochrome ($-NH_2$) on the HAD molecule and chromophore (GA and FA). In addition, effective charge transfer between ligand and metal also can strengthen their light absorption ability. The optical band gaps of Co_2-AW and Co_2-AF determined from the Tauc plot were 1.81 and 1.85 eV (Figure S13), respectively. At the same time, the Mott−Schottky (MS) measurement was implemented to investigate electronic band positions of two BMOFs (Figures S14a,b). LUMO energies of Co_2-AW and Co_2-AF were calculated to be −1.07 and −1.15 V, respectively, while HOMO energies were calculated to be 0.74 (Co_2-AW) and 0.70 V (Co_2-AF). The LUMO levels of these two BMOFs were negative enough for photocatalytic CO_2-to-HCOOH (Figure 2d). Furthermore, ultraviolet photoelectron spectroscopy (UPS) analysis (Figures S14c,d) of these two BMOFs was performed. The HOMO positions of Co_2-AW and Co_2-AF were determined to be 0.72 and 0.69 V, respectively. The corresponding results agreed with that of the LUMO−HOMO energy derived from MS characterization. Obviously, these two BMOFs have excellent UV−vis absorption capacity and negative LUMO energy levels, which are suitable as potential catalysts for CO_2RR. The periodic on/off photocurrent response tests were carried out to investigate photogenerated charge carrier properties (Figure 2c). The results revealed that the photocurrent response of Co_2-AF is stronger than that of Co_2-AW, manifesting its superior photoinduced charge transfer ability promoted by the ferrocene group.

Visible light-driven photocatalytic (CO_2RR) was carried out in acetonitrile with triethylamine (TEA) as the electron donor. HCOOH was the only observed reduction product of CO_2 photoconversion (Figures S15−S17), confirming that these BMOFs catalysts are highly selective. After 10 h, Co_2-AW showed the production of 7.47 μmol of HCOOH (149.4 μmol g^{-1} h^{-1}), while Co_2-AF showed a higher HCOOH yield of 11.29 μmol (225.8 μmol g^{-1} h^{-1}) with visible light irradiation under identical conditions (Figure 3a). The high HCOOH production performance is mainly due to the HAD ligands (including photosensitive units and photocatalytic activation sites) in the BMOFs structure, which was conducive to the catalysts to use more absorbed light and enhance catalytic activity. Moreover, the amino groups of HAD ligands in the homomorphous structures of Co_2-AW and Co_2-AF are pointing to the inner channels and create continuous CO_2

https://doi.org/10.1021/acs.inorgchem.1c03368
Inorg. Chem. 2022, 61, 2167−2173

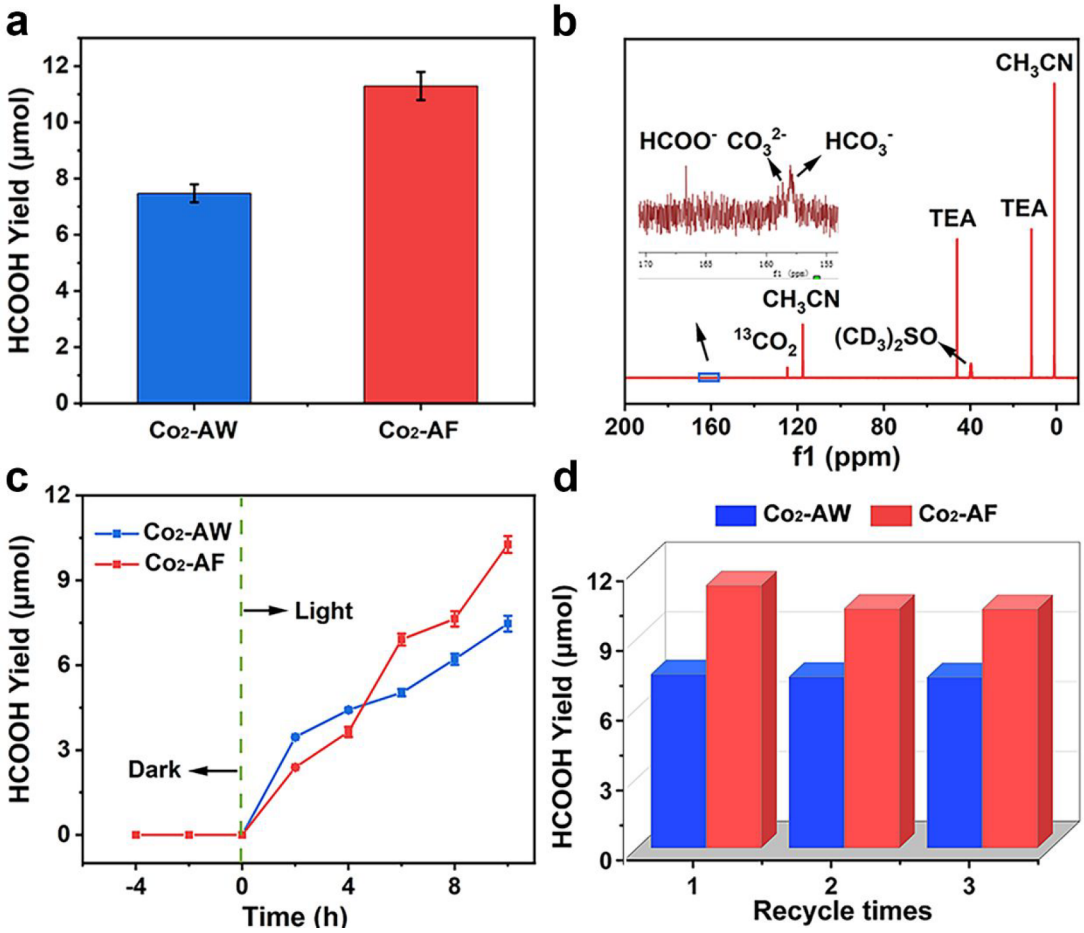

Figure 3. (a) CO_2RR performance of **Co_2-AW** and **Co_2-AF**. (b) ^{13}C NMR spectra of **Co_2-AF** for photocatalytic reduction of $^{13}CO_2$. (c) Amounts of HCOOH produced over time on **Co_2-AW** and **Co_2-AF**. (d) Durability tests of **Co_2-AW** and **Co_2-AF**.

absorption active sites, resulting in high HCOOH yield. Nonetheless, Co_2-AF exhibits a higher photocatalytic activity than Co_2-AW, which is attributed to their superior charge transfer channels provided by the modified FA ligand. The apparent quantum efficiency (QE) was performed, and the results also showed that Co_2-AF has a higher HCOOH yield (see the Supporting Information). Control experiments for photocatalytic CO_2RR activity of these two BMOFs were executed in the absence of photocatalysts, ligand, CO_2, or light illumination. The relevant results were discussed in Table S4. There were no noticeable products detected by ion chromatography (IC) and gas chromatography (GC), evidencing that these BMOFs indeed can finish the photocatalytic CO_2 reduction to HCOOH. To ascertain the carbon source of the generated HCOOH, an isotope-labeling experiment using $^{13}CO_2$ was performed (Figures 3b and S18). Thus, the collected reaction solution after photocatalysis was analyzed by ^{13}C NMR spectroscopy. A single peak centered at δ = 167 ppm was detected under a $^{13}CO_2$ atmosphere (Figure 3b), and this signal can be attributed to $H^{13}COO^-$. The same experiment was implemented with a $^{12}CO_2$ atmosphere, but there is no signal in the ^{13}C NMR spectrum (Figures S19 and S20). These results indicated that the reduction product HCOOH indeed originated from CO_2. In the case of photocatalytic CO_2RR with BMOFs catalysts, the capacity of HCOOH formation was monitored through ion chromatography (IC) at different irradiation time, and it was shown that the catalytic yield can be raised by increasing the irradiation time (Figure 3c). The reaction durability of these BMOFs was executed by the recycling experiment (Figure 3d), and at least three cycles can be retained, evidencing clearly that these crystalline photocatalysts are still active under identical reaction conditions. After a photocatalytic reaction, the catalysts were filtrated. PXRD analysis showed that the photocatalysts remain unchanged (Figures S21 and S22). Further, FTIR analysis confirmed that the original materials retained their characteristic groups (Figures S23 and S24), indicating that all the catalysts are stable under reaction conditions, and the supernatant liquid was analyzed by UV−vis absorption; after removal of the catalysts, there is no redundant signal detected in the spectrum (Figures S25 and S26), suggesting that the CO_2 photoconversion is indeed catalyzed by the catalysts, rather than by the decomposition of the materials. Inductively coupled plasma mass spectrometry (ICP-MS) of the filtrate after reaction was also implemented, and the Co ions were determined to be 0.019% (Co_2-AW) and 0.012% (Co_2-AF), respectively. These experimental results reveal that these two BMOFs can efficiently promote photocatalytic CO_2RR. In the present research,[53−55] some active sites of CO_2RR took place on the N atom, which provided a new insight. Based on the above experimental discussion and analysis, the proper mechanism of these two BMOFs as photocatalysts for photocatalytic CO_2RR is that the photocatalytic CO_2RR active site is the pyrimidine nitrogen atom of

https://doi.org/10.1021/acs.inorgchem.1c03368
Inorg. Chem. 2022, 61, 2167−2173

adenine molecules, next to the amino group with assisted activation, rather than Co ions. This result is consistent with our previously reported work.[56]

■ CONCLUSIONS

In conclusion, two BMOFs were synthesized by a biological adenine molecule with low toxicity and used as effective photocatalysts for photocatalytic CO_2RR. It is worth noting that photocatalytic CO_2RR is more likely to occur on the pyrimidine N atom of adenine, adjacent to the amino group. Significantly, the introduction of adenine can serve as light absorbing units and active sites for a strong binding interaction with CO_2 in BMOFs, which exhibit the excellent photocatalytic activity and selectivity for CO_2-to-HCOOH conversion. Moreover, Co_2-AF modified by the ferrocene group with outstanding charge transfer capacity showed higher photocatalytic activity for CO_2-to-HCOOH conversion than that of homomorphous Co_2-AW. This work tells us that photosensitive adenine ligands as active sites and ferrocene groups with effective charge transfer is an effective strategy to promote the light utilization ability, facilitates the approach of photocatalytic CO_2RR, and provides more insight into designing BMOFs to achieve efficient CO_2RR.

■ ASSOCIATED CONTENT

Supporting Information

The Supporting Information is available free of charge at https://pubs.acs.org/doi/10.1021/acs.inorgchem.1c03368.

Detailed information regarding crystallographic data for **Co_2-AW** and **Co_2-AF**, XRD patterns, and more characterizations (PDF)

Accession Codes

CCDC 2112400−2112401 contain the supplementary crystallographic data for this paper. These data can be obtained free of charge via www.ccdc.cam.ac.uk/data_request/cif, or by emailing data_request@ccdc.cam.ac.uk, or by contacting The Cambridge Crystallographic Data Centre, 12 Union Road, Cambridge CB2 1EZ, UK; fax: +44 1223 336033.

■ AUTHOR INFORMATION

Corresponding Authors

Jiang Liu − *Jiangsu Collaborative Innovation Centre of Biomedical Functional Materials, Jiangsu Key Laboratory of New Power Batteries, School of Chemistry and Materials Science, Nanjing Normal University, Nanjing 210023, P. R. China*; Email: liuj@njnu.edu.cn

Ya-Qian Lan − *Jiangsu Collaborative Innovation Centre of Biomedical Functional Materials, Jiangsu Key Laboratory of New Power Batteries, School of Chemistry and Materials Science, Nanjing Normal University, Nanjing 210023, P. R. China; School of Chemistry, South China Normal University, Guangzhou 510006, P. R. China*; orcid.org/0000-0002-2140-7980; Email: yqlan@njnu.edu.cn; http://www.yqlangroup.com

Authors

Su-Juan Yao − *Jiangsu Collaborative Innovation Centre of Biomedical Functional Materials, Jiangsu Key Laboratory of New Power Batteries, School of Chemistry and Materials Science, Nanjing Normal University, Nanjing 210023, P. R. China*

Ning Li − *School of Chemical Engineering and Light Industry, Guangdong University of Technology, Guangzhou 510006, P. R. China*

Long-Zhang Dong − *Jiangsu Collaborative Innovation Centre of Biomedical Functional Materials, Jiangsu Key Laboratory of New Power Batteries, School of Chemistry and Materials Science, Nanjing Normal University, Nanjing 210023, P. R. China*; orcid.org/0000-0002-9276-5101

Jing-Jing Liu − *School of Chemistry, South China Normal University, Guangzhou 510006, P. R. China*

Zhi-Feng Xin − *Institute of Molecular Engineering and Applied Chemistry, Anhui University of Technology, Ma'anshan, Anhui 243002, P. R. China*; orcid.org/0000-0001-9080-9695

Dong-Sheng Li − *College of Materials and Chemical Engineering, Hubei Provincial Collaborative Innovation Center for New Energy Microgrid, Key Laboratory of Inorganic Nonmetallic Crystalline and Energy Conversion Materials, China Three Gorges University, Yichang 443002, China*; orcid.org/0000-0003-1283-6334

Shun-Li Li − *Jiangsu Collaborative Innovation Centre of Biomedical Functional Materials, Jiangsu Key Laboratory of New Power Batteries, School of Chemistry and Materials Science, Nanjing Normal University, Nanjing 210023, P. R. China*

Complete contact information is available at: https://pubs.acs.org/10.1021/acs.inorgchem.1c03368

Author Contributions

⊥S.-J.Y. and N.L. contributed equally to this work.

Notes

The authors declare no competing financial interest.

■ ACKNOWLEDGMENTS

This work was financially supported by NSFC (Nos. 21871141, 21871142, 22071109, and 92061101), Project funded by China Postdoctoral Science Foundation (No. 2018M630572), Priority Academic Program Development of Jiangsu Higher Education Institutions, and the Foundation of Jiangsu Collaborative Innovation Center of Biomedical Functional Materials.

■ REFERENCES

(1) Cai, H.; Huang, Y.-L.; Li, D. Biological Metal-Organic Frameworks: Structures, Host-Guest Chemistry and Bio-Applications. *Coord. Chem. Rev.* **2019**, *378*, 207−221.

(2) Yang, J.; Li, K.; Li, C.; Gu, J. Intrinsic Apyrase-Like Activity of Cerium-Based Metal-Organic Frameworks (MOFs): Dephosphorylation of Adenosine Tri- and Diphosphate. *Angew. Chem., Int. Ed.* **2020**, *59* (51), 22952−22956.

(3) Chen, S.; Zhu, C.; Xian, W.; Liu, X.; Liu, X.; Zhang, Q.; Ma, S.; Sun, Q. Imparting Ion Selectivity to Covalent Organic Framework Membranes Using de Novo Assembly for Blue Energy Harvesting. *J. Am. Chem. Soc.* **2021**, *143* (25), 9415−9422.

(4) Ye, T.; Hou, G.; Li, W.; Wang, C.; Yi, K.; Liu, N.; Liu, J.; Huang, S.; Gao, J. Artificial Sodium-Selective Ionic Device Based on Crown-Ether Crystals with Subnanometer Pores. *Nat. Commun.* **2021**, *12* (1), 5231.

(5) An, J.; Geib, S. J.; Rosi, N. L. Cation-Triggered Drug Release from a Porous Zinc-Adeninate Metal-Organic Framework. *J. Am. Chem. Soc.* **2009**, *131* (24), 8376−8377.

(6) Ribeiro, A. P. C.; Martins, L. M. D. R. S.; Pombeiro, A. J. L. N_2O-Free Single-Pot Conversion of Cyclohexane to Adipic Acid

Catalysed by an Iron(ii) Scorpionate Complex. *Green Chem.* **2017**, *19* (6), 1499−1501.
(7) Chen, J.; Gong, X.; Li, J.; Li, Y.; Ma, J.; Hou, C.; Zhao, G.; Yuan, W.; Zhao, B. Carbonyl Catalysis Enables a Biomimetic Asymmetric Mannich Reaction. *Science* **2018**, *360* (6396), 1438−1442.
(8) Peng, M.; Wen, Z.; Xie, L.; Cheng, J.; Jia, Z.; Shi, D.; Zeng, H.; Zhao, B.; Liang, Z.; Li, T.; Jiang, L. 3D Printing of Ultralight Biomimetic Hierarchical Graphene Materials with Exceptional Stiffness and Resilience. *Adv. Mater.* **2019**, *31* (35), No. 1902930.
(9) Quan, Y.; Song, Y.; Shi, W.; Xu, Z.; Chen, J. S.; Jiang, X.; Wang, C.; Lin, W. Metal-Organic Framework with Dual Active Sites in Engineered Mesopores for Bioinspired Synergistic Catalysis. *J. Am. Chem. Soc.* **2020**, *142* (19), 8602−8607.
(10) Huang, Y.; Jian, Y.; Li, L.; Li, D.; Fang, Z.; Dong, W.; Lu, Y.; Luo, B.; Chen, R.; Yang, Y.; Chen, M.; Shi, W. A NIR-Responsive Phytic Acid Nickel Biomimetic Complex Anchored on Carbon Nitride for Highly Efficient Solar Hydrogen Production. *Angew. Chem., Int. Ed.* **2021**, *60* (10), 5245−5249.
(11) Chen, R.; Zhuang, G.-L.; Wang, Z.-Y.; Gao, Y.-J.; Li, Z.; Wang, C.; Zhou, Y.; Du, M.-H.; Zeng, S.; Long, L.-S.; Kong, X.-J.; Zheng, L.-S. Integration of Bio-Inspired Lanthanide-Transition Metal Cluster and P-doped Carbon Nitride for Efficient Photocatalytic Overall Water Splitting. *Natl. Sci. Rev.* **2021**, *8* (9), nwaa234.
(12) Liu, G.; Wong, W. S. Y.; Kraft, M.; Ager, J. W.; Vollmer, D.; Xu, R. Wetting-Regulated Gas-Involving (Photo)Electrocatalysis: Biomimetics in Energy Conversion. *Chem. Soc. Rev.* **2021**, *50*, 10674.
(13) Zhang, W.; Nafady, A.; Shan, C.; Wojtas, L.; Chen, Y. S.; Cheng, Q.; Zhang, X. P.; Ma, S. Functional Porphyrinic Metal-Organic Framework as a New Class of Heterogeneous Halogen Bond Donor Catalyst. *Angew. Chem., Int. Ed.* **2021**, *60*, 24312.
(14) Li, T.; Sullivan, J. E.; Rosi, N. L. Design and Preparation of a Core-Shell Metal-Organic Framework for Selective CO_2 Capture. *J. Am. Chem. Soc.* **2013**, *135* (27), 9984−9987.
(15) An, J.; Fiorella, R. P.; Geib, S. J.; Rosi, N. L. Synthesis, Structure, Assembly, and Modulation of the CO_2 Adsorption Properties of a Zinc-Adeninate Macrocycle. *J. Am. Chem. Soc.* **2009**, *131* (24), 8401−8403.
(16) Xie, Z.; Li, T.; Rosi, N. L.; Carreon, M. A. Alumina-Supported Cobalt-Adeninate MOF Membranes for CO_2/CH_4 Separation. *J. Mater. Chem. A* **2014**, *2* (5), 1239−1241.
(17) Li, J.; Jiang, L.; Chen, S.; Kirchon, A.; Li, B.; Li, Y.; Zhou, H. C. Metal-Organic Framework Containing Planar Metal-Binding Sites: Efficiently and Cost-Effectively Enhancing the Kinetic Separation of C_2H_2/C_2H_4. *J. Am. Chem. Soc.* **2019**, *141* (9), 3807−3811.
(18) Zeng, H.; Xie, X. J.; Xie, M.; Huang, Y. L.; Luo, D.; Wang, T.; Zhao, Y.; Lu, W.; Li, D. Cage-Interconnected Metal-Organic Framework with Tailored Apertures for Efficient C_2H_6/C_2H_4 Separation under Humid Conditions. *J. Am. Chem. Soc.* **2019**, *141* (51), 20390−20396.
(19) Weng, H.; Xu, X.-Y.; Yan, B. Novel Multi-Component Photofunctional Nanohybrids for Ratio-Dependent Oxygen Sensing. *J. Colloid Interface Sci.* **2017**, *502*, 8−15.
(20) Zhang, Y.; Mei, J.; Yan, C.; Liao, T.; Bell, J.; Sun, Z. Bioinspired 2D Nanomaterials for Sustainable Applications. *Adv. Mater.* **2020**, *32* (18), No. 1902806.
(21) Chen, K.; Wu, C.-D. Designed Fabrication of Biomimetic Metal-Organic Frameworks for Catalytic Applications. *Coord. Chem. Rev.* **2019**, *378*, 445−465.
(22) An, J.; Farha, O. K.; Hupp, J. T.; Pohl, E.; Yeh, J. I.; Rosi, N. L. Metal-Adeninate Vertices for the Construction of an Exceptionally Porous Metal-Organic Framework. *Nat. Commun.* **2012**, *3* (1), 604.
(23) Morrow, S. M.; Colomer, I.; Fletcher, S. P. A Chemically Fuelled Self-Replicator. *Nat. Commun.* **2019**, *10* (1), 1011.
(24) Naskar, S.; Guha, R.; Muller, J. Metal-Modified Nucleic Acids: Metal-Mediated Base Pairs, Triples, and Tetrads. *Angew. Chem., Int. Ed.* **2020**, *59* (4), 1397−1406.
(25) Müller, J. Nucleic Acid Duplexes with Metal-Mediated Base Pairs and their Structures. *Coord. Chem. Rev.* **2019**, *393*, 37−47.
(26) Sandmann, N.; Defayay, D.; Hepp, A.; Muller, J. Metal-Mediated Base Pairing in DNA Involving the Artificial Nucleobase Imidazole-4-Carboxylate. *J. Inorg. Biochem.* **2019**, *191*, 85−93.
(27) Mandal, S.; Muller, J. Metal-Mediated DNA Assembly with Ligand-Based Nucleosides. *Curr. Opin. Chem. Biol.* **2017**, *37*, 71−79.
(28) Zhang, M.; Gu, Z.-Y.; Bosch, M.; Perry, Z.; Zhou, H.-C. Biomimicry in Metal-Organic Materials. *Coord. Chem. Rev.* **2015**, *293−294*, 327−356.
(29) Burneo, I.; Stylianou, K. C.; Rodríguez-Hermida, S.; Juanhuix, J.; Fontrodona, X.; Imaz, I.; Maspoch, D. Two New Adenine-Based Co(II) Coordination Polymers: Synthesis, Crystal Structure, Coordination Modes, and Reversible Hydrochromic Behavior. *Cryst. Growth Des.* **2015**, *15* (7), 3182−3189.
(30) Verma, S.; Mishra, A. K.; Kumar, J. The Many Facets of Adenine: Coordination, Crystal Patterns, and Catalysis. *Acc. Chem. Res.* **2010**, *43* (1), 79−91.
(31) Verma, S.; Mishra, A. K.; Kumar, J. The many Facets of Adenine: Coordination, Crystal Patterns, and Catalysis. *Acc. Chem. Re.s* **2010**, *43* (1), 79−91.
(32) Li, T.; Chen, D.-L.; Sullivan, J. E.; Kozlowski, M. T.; Johnson, J. K.; Rosi, N. L. Systematic Modulation and Enhancement of CO_2: N_2 Selectivity and Water Stability in an Isoreticular Series of Bio-MOF-11 Analogues. *Chem. Sci.* **2013**, *4* (4), 1746−1755.
(33) Zhuo, T. C.; Song, Y.; Zhuang, G. L.; Chang, L. P.; Yao, S.; Zhang, W.; Wang, Y.; Wang, P.; Lin, W.; Lu, T. B.; Zhang, Z. M. H-Bond-Mediated Selectivity Control of Formate versus CO during CO_2 Photoreduction with Two Cooperative Cu/X Sites. *J. Am. Chem. Soc.* **2021**, *143* (16), 6114−6122.
(34) Cai, H.; Li, M.; Lin, X. R.; Chen, W.; Chen, G. H.; Huang, X. C.; Li, D. Spatial, Hysteretic, and Adaptive Host-Guest Chemistry in a Metal-Organic Framework with Open Watson-Crick Sites. *Angew. Chem., Int. Ed.* **2015**, *54* (36), 10454−9.
(35) Li, N.; Liu, J.; Dong, B. X.; Lan, Y. Q. Polyoxometalate-Based Compounds for Photo- and Electrocatalytic Applications. *Angew. Chem., Int. Ed.* **2020**, *59* (47), 20779−20793.
(36) Luo, Y.-H.; Dong, L.-Z.; Liu, J.; Li, S.-L.; Lan, Y.-Q. From Molecular Metal Complex to Metal-Organic Framework: The CO_2 Reduction Photocatalysts with Clear and Tunable Structure. *Coord. Chem. Rev.* **2019**, *390*, 86−126.
(37) Li, D.; Kassymova, M.; Cai, X.; Zang, S.-Q.; Jiang, H.-L. Photocatalytic CO_2 Reduction over Metal-Organic Framework-Based Materials. *Coord. Chem. Rev.* **2020**, *412*, 213262.
(38) Li, N.; Liu, J.-J.; Sun, J.-W.; Dong, B.-X.; Dong, L.-Z.; Yao, S.-J.; Xin, Z.; Li, S.-L.; Lan, Y.-Q. Calix[8]arene-Constructed Stable Polyoxo-Titanium Clusters for Efficient CO_2 Photoreduction. *Green Chem.* **2020**, *22* (16), 5325−5332.
(39) Wang, Y.; Shang, X.; Shen, J.; Zhang, Z.; Wang, D.; Lin, J.; Wu, J. C. S.; Fu, X.; Wang, X.; Li, C. Direct and Indirect Z-scheme Heterostructure-Coupled Photosystem Enabling Cooperation of CO_2 Reduction and H_2O Oxidation. *Nat. Commun.* **2020**, *11* (1), 3043.
(40) Li, X. X.; Zhang, L.; Liu, J.; Yuan, L.; Wang, T.; Wang, J. Y.; Dong, L. Z.; Huang, K.; Lan, Y. Q. Design of Crystalline Reduction-Oxidation Cluster-Based Catalysts for Artificial Photosynthesis. *JACS Au.* **2021**, *1* (8), 1288−1295.
(41) Li, H.; Zhang, J.; Yu, J.; Cao, S. Ultra-Thin Carbon-Doped Bi_2WO_6 Nanosheets for Enhanced Photocatalytic CO_2 Reduction. *Trans. Tianjin Univ.* **2021**, *27* (4), 338−347.
(42) Xiong, X.; Mao, C.; Yang, Z.; Zhang, Q.; Waterhouse, G. I. N.; Gu, L.; Zhang, T. Photocatalytic CO_2 Reduction to CO over Ni Single Atoms Supported on Defect-Rich Zirconia. *Adv. Energy Mater.* **2020**, *10* (46), 2002928.
(43) Xiong, X.; Zhao, Y.; Shi, R.; Yin, W.; Zhao, Y.; Waterhouse, G. I. N.; Zhang, T. Selective Photocatalytic CO_2 Reduction over Zn-based Layered Double Hydroxides Containing Tri or Tetravalent Metals. *Sci. Bull.* **2020**, *65* (12), 987−994.
(44) Ribeiro, A. P. C.; Martins, L. M. D. R. S.; Pombeiro, A. J. L. Carbon Dioxide-to-Methanol Single-Pot Conversion Using a C-Scorpionate Iron(ii) Catalyst. *Green Chem.* **2017**, *19* (20), 4811−4815.

(45) Rayder, T. M.; Adillon, E. H.; Byers, J. A.; Tsung, C.-K. A Bioinspired Multicomponent Catalytic System for Converting Carbon Dioxide into Methanol Autocatalytically. *Chem.* **2020**, *6* (7), 1742−1754.
(46) Chen, Y.; Li, P.; Zhou, J.; Buru, C. T.; Dordevic, L.; Li, P.; Zhang, X.; Cetin, M. M.; Stoddart, J. F.; Stupp, S. I.; Wasielewski, M. R.; Farha, O. K. Integration of Enzymes and Photosensitizers in a Hierarchical Mesoporous Metal-Organic Framework for Light-Driven CO_2 Reduction. *J. Am. Chem. Soc.* **2020**, *142* (4), 1768−1773.
(47) Miller, T. E.; Beneyton, T.; Schwander, T.; Diehl, C.; Girault, M.; McLean, R.; Chotel, T.; Claus, P.; Cortina, N. S.; Baret, J.-C.; Erb, T. J. Light-Powered CO_2 Fixation in a Chloroplast Mimic with Natural and Synthetic Parts. *Science* **2020**, *368* (6491), 649−654.
(48) Li, J.; Huang, H.; Xue, W.; Sun, K.; Song, X.; Wu, C.; Nie, L.; Li, Y.; Liu, C.; Pan, Y.; Jiang, H.-L.; Mei, D.; Zhong, C. Self-Adaptive Dual-Metal-Site Pairs in Metal-Organic Frameworks for Selective CO_2 Photoreduction to CH_4. *Nat. Catal.* **2021**, *4* (8), 719−729.
(49) Watanabe, T.; Pfeil-Gardiner, O.; Kahnt, J.; Koch, J.; Shima, S.; Murphy, B. J. Three-Megadalton Complex of Methanogenic Electron-Bifurcating and CO_2-Fixing Enzymes. *Science* **2021**, *373* (6559), 1151−1156.
(50) Liu, J.-J.; Li, N.; Sun, J.-W.; Liu, J.; Dong, L.-Z.; Yao, S.-J.; Zhang, L.; Xin, Z.-F.; Shi, J.-W.; Wang, J.-X.; Li, S.-L.; Lan, Y.-Q. Ferrocene-Functionalized Polyoxo-Titanium Cluster for CO_2 Photoreduction. *ACS Catalysis.* **2021**, *11* (8), 4510−4519.
(51) Jäkle, F.; Sheridan, J. B. Ferrocenes. Ligands, Materials and Biomolecules. Edited by Petr Štěpnička. *Angew. Chem., Int. Ed.* **2008**, *47* (40), 7587−7587.
(52) Xin, Z.; Wang, Y.-R.; Chen, Y.; Li, W.-L.; Dong, L.-Z.; Lan, Y.-Q. Metallocene Implanted Metalloporphyrin Organic Framework for Highly Selective CO_2 Electroreduction. *Nano Energy* **2020**, *67*, 104233.
(53) Sun, S.-N.; Li, N.; Liu, J.; Ji, W.-X.; Dong, L.-Z.; Wang, Y.-R.; Lan, Y.-Q. Identification of the Activity Source of CO_2 Electroreduction by Strategic Catalytic Site Distribution in Stable Supramolecular Structure System. *Natl. Sci. Rev.* **2021**, *8* (3), nwaa195.
(54) Kar, S.; Sen, R.; Kothandaraman, J.; Goeppert, A.; Chowdhury, R.; Munoz, S. B.; Haiges, R.; Prakash, G. K. S. Mechanistic Insights into Ruthenium-Pincer-Catalyzed Amine-Assisted Homogeneous Hydrogenation of CO_2 to Methanol. *J. Am. Chem. Soc.* **2019**, *141* (7), 3160−3170.
(55) He, C.; Zhang, Y.; Zhang, Y.; Zhao, L.; Yuan, L. P.; Zhang, J.; Ma, J.; Hu, J. S. Molecular Evidence for Metallic Cobalt Boosting CO_2 Electroreduction on Pyridinic Nitrogen. *Angew. Chem., Int. Ed.* **2020**, *59* (12), 4914−4919.
(56) Li, N.; Liu, J.; Liu, J. J.; Dong, L. Z.; Xin, Z. F.; Teng, Y. L.; Lan, Y. Q. Adenine Components in Biomimetic Metal-Organic Frameworks for Efficient CO_2 Photoconversion. *Angew. Chem., Int. Ed.* **2019**, *58* (16), 5226−5231.

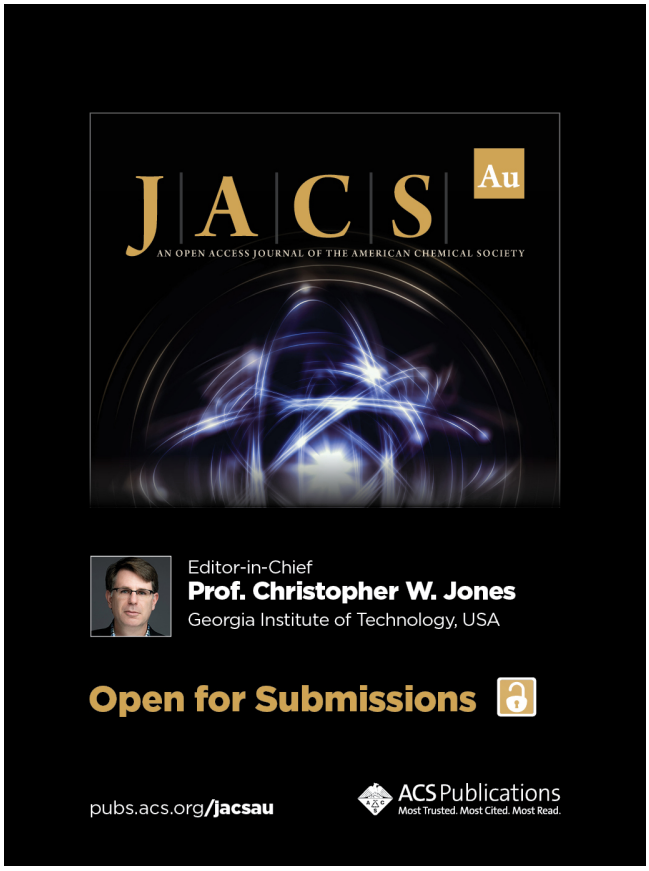

https://doi.org/10.1021/acs.inorgchem.1c03368
Inorg. Chem. 2022, 61, 2167−2173